(27) It is interesting to note that in phase II (α) of PVDF the closest H–F distances are not all to the fluorine atoms on adjacent carbon atoms. The shortest H–F distances of H1, for instance, are to F2 and F3, on adjacent *different* carbon atoms and to F1′ and F2′ on carbons three bonds removed from the carbon to which H1 is connected (see ref 20).
(28) McConnell, H. M.; Holm, C. H. *J. Chem. Phys.* **1956**, *25*, 1289.
(29) Broadhurst, M. G., private communication.
(30) Yoda, O.; Kuriyama, I.; Odajima, A. *J. Mater. Sci. Lett.* **1982**, *1*, 451.
(31) Fujimura, T.; Hayakawa, N.; Kuriyama, I. *J. Appl. Polym. Sci.* **1982**, *27*, 4093.

Aromatic Ring Flips in a Semicrystalline Polymer

Ashok L. Cholli, Joseph J. Dumais, Alan K. Engel,† and Lynn W. Jelinski*
AT&T Bell Laboratories, Murray Hill, New Jersey 07974. *Received February 23, 1984*

ABSTRACT: We report a detailed analysis of the phenyl ring motions that occur in the semicrystalline polymer [aromatic-d_4]poly(butylene terephthalate). Solid-state deuterium NMR results show that there are three distinct motional regimes, consisting of (1) the crystalline regions, where the phenyl rings are static, (2) a region of intermediate mobility, in which the aromatic groups undergo slow 180° ring flips, and (3) the amorphous part, in which the rings undergo 180° flips ($\tau_c = 1.8 \times 10^{-6}$ s at 70 °C) superimposed on rapid, low-angle librational motions. The 180° ring flip process has an activation energy of 5.9 kcal/mol. The amount of each phase is in accord with density measurements. Whether a phenyl ring does or does not undergo a 180° ring flip is attributed to the conformational space surrounding that site. The phenyl ring flip process appears to be universal, occurring here as well as in small organic molecules, other synthetic polymers, and biopolymers. It can be used as a sensitive reporter of morphology in these materials. Pulse sequences are described for the selective observation of separate motional regions in polymers.

A dispersion in the rates of aromatic ring flips has been demonstrated elegantly by Wüthrich and co-workers,[1] who observed by solution-state proton NMR spectroscopy that the aromatic rings in bovine pancreatic trypsin inhibitor have different ring flip rates. These differences in phenyl ring flip rates were originally attributed to biological activity. However, the discovery of aromatic ring flips in the crystalline amino acid phenylalanine[2] suggested that the occurrence of these phenyl motions is not related to biological activity but reflects instead the local structure of the material. Phenyl ring flips have since been observed in several other solid polymers and biopolymers, including the crystalline peptide enkephalin,[3] the amorphous polymer polycarbonate,[4,5] epoxy resins,[6] polystyrene,[5,7] and drawn poly(ethylene terephthalate).[8]

Although phenyl ring flips have now been observed in a number of systems, several fundamental questions concerning aromatic ring flips remain unanswered, particularly in the area of semicrystalline polymers. Among these are the following: (1) Is a pure 180° flip model adequate to explain the motion of phenyl rings in polymers? (2) Do phenyl ring flips occur only in the amorphous regions of semicrystalline polymers? (3) What is the activation energy for a 180° ring flip in a semicrystalline polymer? (4) Is there a homogeneous (narrow) or heterogeneous (broad) distribution of phenyl ring flip rates in these systems?

We report here data bearing on these questions. This work involves a detailed solid-state deuterium NMR study of phenyl ring flips in poly(butylene terephthalate):[9]

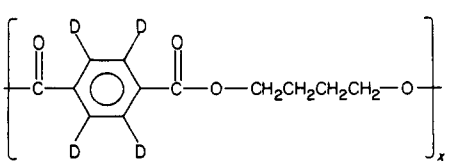

A phenyl ring flip in this system requires rotation about sp^2–sp^2 bonds. The aromatic and carbonyl groups participate in π-bond conjugation, causing the carbonyl–aromatic bonds to have partial double-bond character. The carbonyl groups and the intervening aromatic ring therefore tend to be coplanar. This aromatic system is predicted to have two predominant conformations, interconvertable by 180° flips.[10]

Deuterium NMR spectroscopy in the solid state is well suited for determining the details of local molecular motions in polymers.[5,11] The deuterium NMR spectrum of a static C–D bond (i.e., one that is not undergoing motion on the deuterium NMR time scale and has a correlation time $\tau_c > 10^{-3}$ s) consists of a Pake doublet that has a quadrupole splitting, $\Delta\nu_q$, of 128 kHz ($\Delta\nu_q$ is three-quarters of the quadrupole coupling constant, or $3e^2Qq/4h$). The electric field gradient tensor is axially symmetric, which means that there is a one-to-one correspondence between the orientation of the C–D bond with respect to the magnetic field and the frequency at which this orientation resonates. Furthermore, the symmetry axis of the field gradient tensor is along the C–D bond axis. Because the field gradient tensor is axially symmetric and since the molecular orientation of the principal axes of the field gradient tensor is known, the interpretation of deuterium line shapes in the presence of motion becomes straightforward.[5,11] In addition to depending on the jump angle for motion, deuterium NMR line shapes are also sensitive to the correlation time for motion when the correlation time is in the intermediate exchange regime (10^{-8} s $< \tau_c < 10^{-4}$ s).[11] Therefore, temperature-dependent solid-state deuterium NMR spectra can be used to extract information concerning both the *rate* and *angular range* of local polymer motions. Finally, measurements of spin–lattice relaxation times can also be used to verify the correlation times determined from the line shape analyses and can also be used to determine correlation times when the line shape is no longer sensitive to increased motional rates ($\tau_c < 10^{-8}$ s).[12]

Explicit examples of the deuterium NMR line shapes that are predicted for the deuterated aromatic ring of poly(butylene terephthalate) are shown in Figure 1. If the aromatic rings are static on the deuterium NMR time

† E. I. du Pont de Nemours and Co., Wilmington, DE 19898; current address: Sophia University, Tokyo 102, Japan.

0024-9297/84/2217-2399$01.50/0

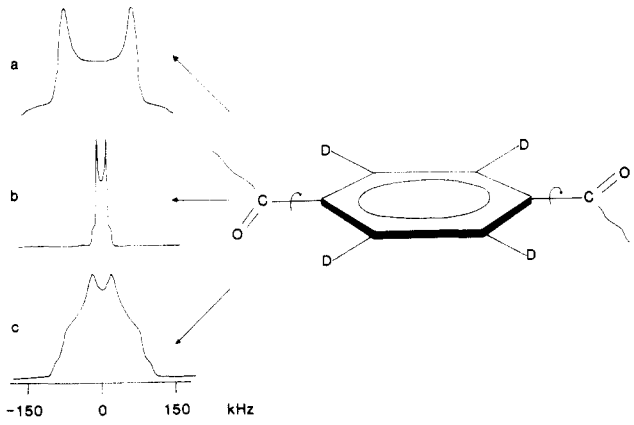

Figure 1. Predicted ^2H NMR spectra for possible phenyl motions representing (a) static powder pattern with a quadrupole coupling constant of 156 kHz (the splitting between perpendicular edges is 128 kHz), (b) powder pattern for fast continuous diffusion about the 1,4-phenylene axis. (the splitting between perpendicular edges is one-eighth of the static powder pattern splitting), and (c) powder pattern for fast 180° phenyl ring flips, (the separation between the inner two peaks is one-fourth of the static pattern splitting).

scale, the observed pattern will be the Pake spectrum shown in Figure 1a, with a 128-kHz splitting between the singularities. If the aromatic rings are involved in rapid continuous diffusion about the carbonyl–aromatic bond, the Pake pattern is predicted to collapse by a factor of $(3\cos^2\theta - 1)/2$, where θ is the angle (60°) that the C–D bond makes with the rotation axis. This spectrum with its 16-kHz quadrupole splitting is shown in Figure 1b. If instead the aromatic rings undergo discrete 180° flips about the carbonyl–aromatic bond, the predicted line shape would be the one shown in Figure 1c. The positions of the singularities corresponding to the motionally averaged pattern in Figure 1c can be calculated by considering the effect that a 180° phenyl ring flip has on the components of the field gradient tensor.[3] The tensor component perpendicular to the C–D bond is not averaged by this motion and remains at ω = 128/2 or 64 kHz. The 180° ring flip causes the tensor component parallel to the C–D bond to jump between two orientations separated by 120°. This motionally averaged component can be calculated by the same arguments used to calculate the rapid diffusion case, above, and occurs at 16 kHz. Because the tensor must remain traceless, the third component must occur at -80 kHz. The deuterium NMR line shape observed for aromatic rings undergoing rapid 180° ring flips thus has a total width of 160 kHz and distinct singularities separated by 32 kHz (Figure 1c).

Experimental Section

Sample. The selectively labeled [aromatic-d_4]poly(butylene terephthalate) sample was prepared according to literature methods,[13] using dimethyl [aromatic-d_4]terephthalate (Merck Isotopes) as the starting terephthalate ester. The T_g is 50 °C, measured on a DuPont 1090 DSC with a heating rate of 10 °C/min. The labeled polymer was also characterized by solution-state deuterium and carbon-13 NMR spectroscopy. The deuterium NMR spectra attested to the integrity of the labeling pattern and the carbon-13 spectra showed that no low-molecular-weight impurities are present in the sample. Density measurements were performed by flotation methods.[14]

The sample for solid-state deuterium NMR measurements was melted into a 5 mm × 15 mm o.d. glass tube and allowed to cool from the melt. The sample weight was approximately 100 mg. All temperature-dependent changes in the NMR line shape were fully reversible with temperature cycling.

NMR Measurements. Solid-state deuterium NMR spectra were obtained on a home-built spectrometer operating at 55.26 MHz for deuterium. The spectrometer has been described previously.[15] The sample temperature was regulated by using either a heated air flow or a liquid nitrogen boil-off system. The temperatures were measured by means of a digital thermometer (Omega 2176A) with a copper–constantan thermocouple. Temperatures are considered accurate and stable to ±1 °C.

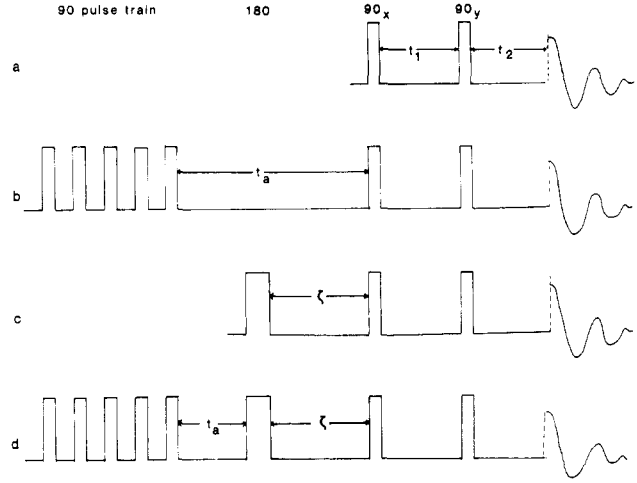

Figure 2. Solid-state ^2H NMR pulse sequences: (a) quadrupole echo pulse sequence; (b) amorphous quadrupole echo pulse sequence; (c) inversion–recovery quadrupole echo pulse sequence; (d) amorphous inversion–recovery quadrupole echo pulse sequence. The pulse widths and optimum delay times are described in the text. These pulse sequences do not show the recycle delay time, T.

The 90° pulse width was typically 3.2 μs. Data were collected in quadrature using 4K points and a sampling rate of 100 ns/point. The FID was zero-filled to 8K prior to Fourier transformation.

Pulse Sequences. Different pulse sequences were used to observe selectively different regions (i.e., crystalline, interphase, or amorphous) of the polymer. The pulse sequences are shown in Figure 2 and are described here in brief.

The *quadrupolar echo pulse sequence*[16-18] (Figure 2a) ($90_{\pm x}$–t_1–90_y–t_2–acquire–T) was used to obtain most of the solid-state deuterium NMR spectra. This sequence provides a method to refocus the rapidly decaying deuterium signal while the receiver recovers from the high-power transmitter pulse. The delay times t_1 and t_2 were set at 30 and 25 μs, respectively. The FID that is obtained with these delay times is left-shifted so that the part of the FID that is transformed begins at the exact top of the echo maximum. At long recycle delay times (T = 60 s), the spectra represent contributions from both the crystalline and noncrystalline regions of the polymer. Spectra obtained at shorter recycle delay times (T = 1–2 s) arise primarily from the noncrystalline regions.

The *amorphous quadrupole echo pulse sequence* (90–2 ms)$_5$–t_a–$90_{\pm x}$–t_1–90_y–t_2–acquire–T) (Figure 2b) provides an effective way to obtain a solid-state deuterium NMR spectrum of the amorphous component of the semicrystalline polymer. This pulse sequence consists of three parts: (a) a 90° pulse train to saturate the entire spin system, (b) a delay t_a to allow the amorphous deuterons to relax, and (c) the regular quadrupolar echo pulse sequence. The optimum delay time t_a is generally 3 times longer than the T_1 of the amorphous deuterons. The train of 90° pulses is more effective in suppressing signals from the crystalline region than is a single 90° or 180° pulse because of the problems associated with performing a perfect pulse over the ~250-kHz width of the spectrum.

The *inversion–recovery quadrupole echo pulse sequence* (180–τ–$90_{\pm x}$–t_1–90_y–t_2–acquire–T) (Figure 2c) was used to measure some of the solid-state deuterium NMR spin–lattice relaxation times. The first 180° pulse orients the deuteron magnetization along the $-z$ direction. During the variable period τ, deuteron spin–lattice relaxation processes occur and the remaining magnetization is monitored by the quadrupole echo pulse sequence.

Spin–lattice relaxation times for the amorphous deuterons in semicrystalline polymers can be measured selectively by using the *amorphous inversion–recovery quadrupole echo pulse se-*

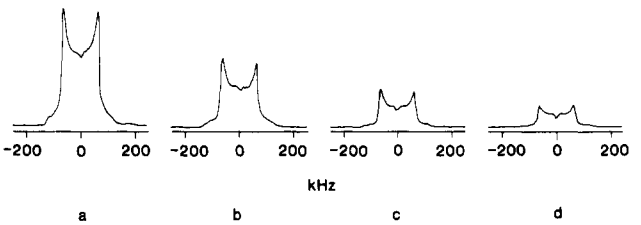

Figure 3. Experimental solid-state ^2H NMR spectra of [aromatic-d_4]poly(butylene terephthalate). (a–c) Spectra obtained with the quadrupole echo pulse sequence with recycle delay time 60, 10, and 1 s, respectively; (d) spectrum obtained with the amorphous quadrupole echo pulse sequence. The interval t_a in the amorphous quadrupole echo experiment was 350 ms for the spectrum in (d). The spectra are plotted so that the intensities are directly comparable.

quence ((90–2 ms)$_5$–t_a–180–τ–90$_{\pm x}$–t_1–90$_y$–t_2–acquire–T) (Figure 2d). The entire spin system is presaturated by the train of 90° pulses. The amorphous deuterons relax during the t_a delay, and the amorphous deuteron magnetization is then inverted by the following 180° pulse, allowed to relax during the variable τ delay, and monitored by the quadrupole echo sequence.

Data Analysis. Spin–lattice relaxation times either were estimated from the null point in a series of inversion–recovery spectra or were determined from progressive saturation experiments. The point in the spectrum used for intensity measurements corresponds to the frequency position from those orientations of the C–D bond that are perpendicular to the magnetic field (i.e., $\omega_\perp$). The inversion–recovery spectra showed a small amount of anisotropy across the powder pattern, as expected.[11,12]

Calculated solid-state deuterium NMR spectra were obtained according to the methods described by Mehring.[19] The calculated spectra have been corrected for pulse power fall-off as a function of frequency[20] and for motions that occur during the quadrupole echo delay time.[21]

Results

General Description of Spectra. Representative quadrupole echo solid-state deuterium NMR spectra for aromatic-deuterated poly(butylene terephthalate) at 23 °C are shown in Figure 3. The pulse sequence recycle delay times are 60 s in (a), 10 s (b), and 1 s in (c). The spectrum in (d) was obtained with the amorphous quadrupole echo pulse sequence. The spectrum obtained with a 60-s recycle delay time exhibits full intensity for both the crystalline and noncrystalline components. Because this material is highly crystalline (ca. 70%), the signals from the aromatic rings in the crystalline environments almost completely mask the signals from the amorphous regions. Figure 3 shows that as the recycle delay time is decreased (i.e., in going from (a) to (c)), more of the amorphous and less of the crystalline rings contribute to the spectrum. It is estimated from a series of spectra such as these that the spin–lattice relaxation time (T_1) for the deuterons on the aromatic rings in the crystalline regions is ca. 15 s at 23 °C.

The spectrum on the far right of Figure 3 was obtained with the amorphous quadrupole echo pulse sequence (see Experimental Section) and represents predominantly the amorphous deuterons. The differences observed between this spectrum and the quadrupole echo spectrum obtained with a 1-s recycle delay are attributed to deuterons of intermediate mobility (i.e., deuterons with mobilities between those of the crystalline and amorphous regions).

Figure 4 shows representative spectra obtained at 70 °C, illustrating that a combination of pulse sequences and subtraction techniques can be used to extract spectra that represent primarily the crystalline, the interphase, and the amorphous regions. The pulse sequences and subtractions used to obtain the spectra in the "difference" column of Figure 4 are described in detail in the figure caption. The

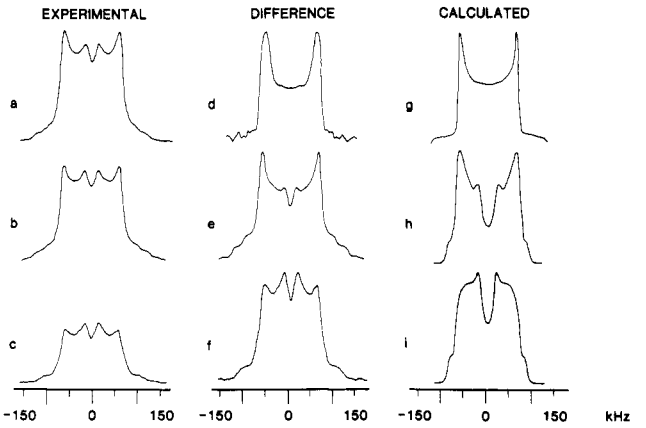

Figure 4. (a–c) Solid-state ^2H NMR spectra of [aromatic-d_4]-poly(butylene terephthalate) at 70 °C. Spectra a and b are obtained with the quadrupole echo pulse sequence with recycle times of 60 and 1 s, respectively. Spectrum c is obtained with the amorphous quadrupole echo pulse sequence. Difference spectrum (d) = (a) – (b) represents primarily the crystalline region of the semicrystalline polymer. Difference spectrum (e) = (b) – (c) represents the interphase region of the polymer. Spectrum f is the same as spectrum c but is shown at a different gain. Spectra g–i are calculated spectra. The calculated spectra assume a 156-kHz quadrupole coupling constant and a 180° phenyl ring flip. The rate constants used in calculated spectra are (g) 9.48 × 10^2, (h) 1.23 × 10^5, and (i) 5.68 × 10^5 s^{-1}.

calculated spectra shown in Figure 4 were obtained by the methods outlined in the Experimental Section and are discussed in following sections.

Taken together, spectra such as those in Figures 3 and 4 show that although semicrystalline poly(butylene terephthalate) is a complicated system from a spectroscopic point of view, various pulse sequences and subtraction methods can be used to simplify the spectra and to extract explicit information.

Spectra Representing the Amorphous Deuterons. A complete series of variable-temperature solid-state deuterium NMR spectra were obtained for the amorphous component of poly(butylene terephthalate) by using the amorphous quadrupole echo pulse sequence (see Experimental Section). Representative spectra are shown in Figures 5 and 6.

The solid-state deuterium NMR spectrum of the amorphous deuterons at −60 °C (not shown) is that of a static quadrupolar powder pattern. The splitting between the singularities, $\Delta\nu_q$, is 128 kHz. The line shapes undergo marked changes as the temperature is increased. At +70 °C the line shape is similar to that predicted for rapid 180° ring flips (see Figure 1c). At the highest temperature observed (96 °C), the line shape shows additional sharp features in the center. The relaxation data for the amorphous deuterons (see below) show that these sharp features represent deuterons undergoing more nearly isotropic reorientation. A full description and interpretation of the calculated spectra will be deferred to the Discussion.

Relaxation Measurements. The spin–lattice relaxation time (T_1) for the aromatic deuterons in the crystalline regions of poly(butylene terephthalate) was estimated from progressive-saturation type experiments shown in Figure 3. Spin–lattice relaxation times for the amorphous deuterons were measured by using the pulse sequence shown in Figure 2d and estimated from the null points in the spectra. The T_1 data are summarized in Table I. Representative plots of the T_1 data for the amorphous deuterons at two temperatures are shown in Figure 7. The T_1 is somewhat anisotropic across the powder pattern, as expected.[11,12] This is particularly noticeable in Figure 7a,

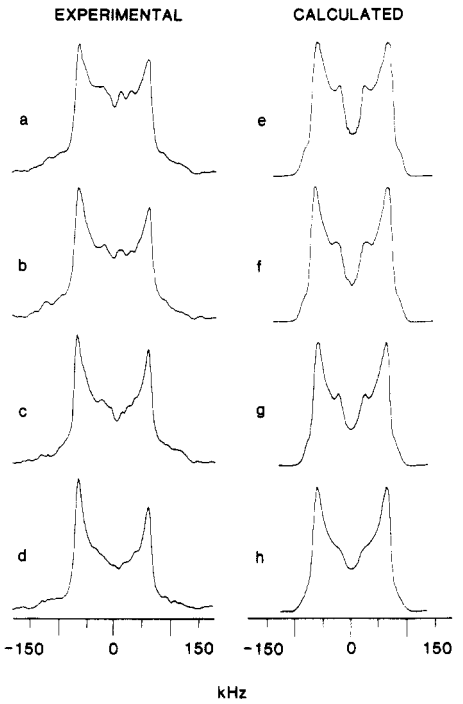

Figure 5. Experimental (a–d) and calculated (e–h) solid-state ^2H NMR spectra representing the amorphous deuterons of [aromatic-d_4]poly(butylene terephthalate). Spectra a–d were obtained with the amorphous quadrupole echo pulse sequence at +10, 0, −10, and −20 °C, respectively. The rate constants for the calculated spectra are (e) 9.48×10^4, (f) 5.68×10^4, (g) 5.2×10^4, and (h) 2.84×10^4 s^{-1}.

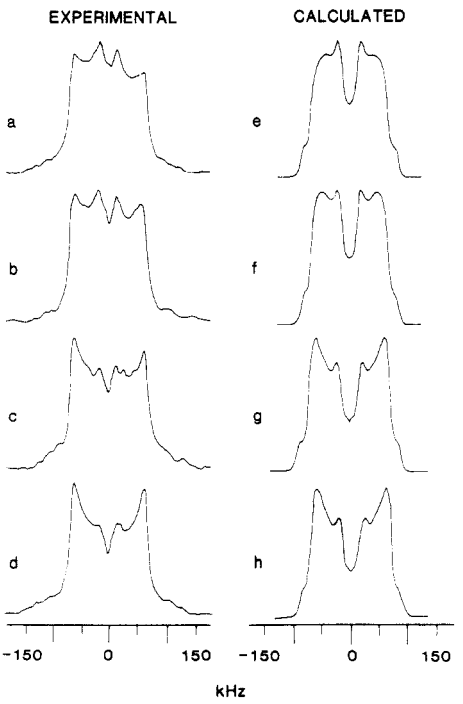

Figure 6. Experimental and calculated solid-state ^2H NMR spectra as described in the legend for Figure 5: (a) 70, (b) 50, (c) 30, and (d) 22 °C; rate constants: (e) 5.68×10^5, (f) 3.8×10^5, (g) 1.8×10^5, (h) 1.52×10^5 s^{-1}.

in which the perpendicular singularities invert at a rate different from that of the middle of the pattern. In view of the multicomponent nature of the line shapes we feel that a more precise analysis of these data would be premature. Furthermore, the inversion–recovery spectra obtained at 96 °C clearly show that at least two components contribute to the amorphous spectrum obtained at this temperature. These spin–lattice relaxation studies further emphasize the wide range of motional heterogeneity observed in these systems.

Table I
Spin–Lattice Relaxation Times (T_1) for the Aromatic Deuterons in Poly(butylene terephthalate)

	T_1, s	
temp, °C	amorphous[a]	crystalline[b]
23	0.110	15
70	0.036	
96	0.007	

[a] Determined at 55.26 MHz using the pulse sequence shown in Figure 2d. The T_1 values are estimated from the null points. [b] Estimated from progressive-saturation measurements at 55.26 MHz.

Table II
Poly(butylene terephthalate) Composition

	by NMR[a]	by density[b]
crystalline	69	75
interphase	9	
amorphous	22	

[a] Determination method described in text. [b] Determined by flotation.[14]

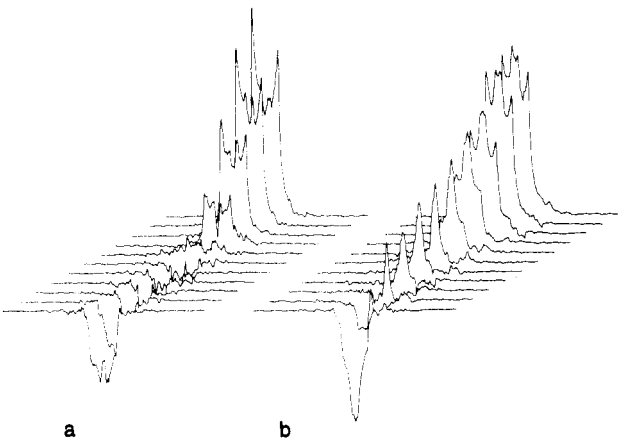

Figure 7. Stacked plots for T_1 measurements using the amorphous inversion–recovery quadrupole echo pulse sequence at (a) 23 and (b) 96 °C. The variable delay τ in these plots is (from bottom to top) 1, 10, 20, 30, 40, 50, 100, 200, 400, 800, and 1000 ms.

Discussion

Morphology. The solid-state deuterium NMR spectra shown in Figures 3 and 4 provide strong evidence for the existence of three motional regions in poly(butylene terephthalate). The region of intermediate mobility is attributed to an "interphase" region, in which the restriction of motion is due to proximity to the crystalline regions. The amount of each region can be estimated by integration of the deuterium NMR spectra shown in Figure 4. These data are listed in Table II, where they are compared to the results of density measurements. Although the density measurements and NMR data are in good agreement, it should be stressed that solid-state deuterium NMR spectra are subject to intensity distortions when the motions are in the intermediate-exchange region.[21] Therefore, the data and methodology presented here must be considered as estimates.

There is precedent for the presence of more than two phases in semicrystalline polymers. Other workers have observed three morphological phases in polyethylene,[22–24] which they describe as a crystalline one, a noncrystalline region with liquid-like character, and an intermediate phase where molecular motion is partly hindered. The

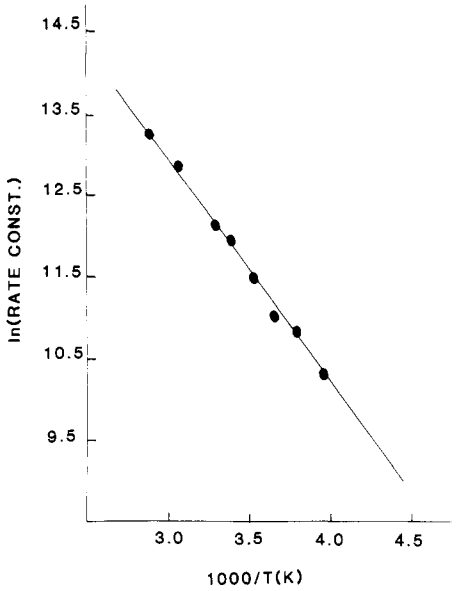

Figure 8. Arrhenius plot of the natural logarithm of the rate constants vs. $1/T$. An apparent activation energy of 5.9 kcal/mol is obtained from the slope of this plot.

three regions observed here can be described somewhat differently. The calculated spectra in Figure 4 show that the three regions in poly(butylene terephthalate) consist of a crystalline region in which phenyl rings are static, an amorphous region in which the aromatic rings undergo (primarily) rapid 180° ring flips, and an intermediate region in which the aromatic rings undergo very slow 180° flips. Analysis of the 180° ring flips in the amorphous regions will be described in detail in the next section.

It should also be noted that categorizing the phenyl ring motions into three distinct groups—crystalline, intermediate, and amorphous—is artificial. All of the solid-state deuterium NMR data suggest that there is a heterogeneous distribution of phenyl ring motions in poly(butylene terephthalate), rather than several discrete regions of motion. In particular, the use of a two-phase model (amorphous plus interphase) to characterize the noncrystalline regions is an idealization. Our data do not allow us to distinguish between this model and a broad distribution of correlation times. Whether or not a particular phenyl ring undergoes a ring flip appears to be related to the conformational space available for the flipping process.

Molecular Motion in the Amorphous Regions. The calculated spectra shown in Figures 5 and 6 were obtained by assuming that the aromatic rings in the amorphous region undergo pure 180° ring flips and that the rate of these flips changes with temperature. The calculated and experimental spectra are in fair agreement, particularly for the low-temperature spectra. However, the centers of the experimental spectra are more filled-in than predicted, and the expected definition at the edges of the powder patterns is lost. These observations are consistent with the presence of additional high-frequency librational motions (root-mean-square deviation estimated to be ±15°) that are superimposed on the 180° phenyl ring flips. The conclusion that can be made by comparing the experimental and calculated spectra in Figures 5 and 6 is that the *primary* mode of motion is well explained by 180° phenyl ring flips but that other phenyl motions are also present. The spectra obtained at high temperatures (e.g., Figure 7) show the existence of more than one type of phenyl motional environment, again emphasizing the heterogeneous nature of phenyl motions in poly(butylene terephthalate).

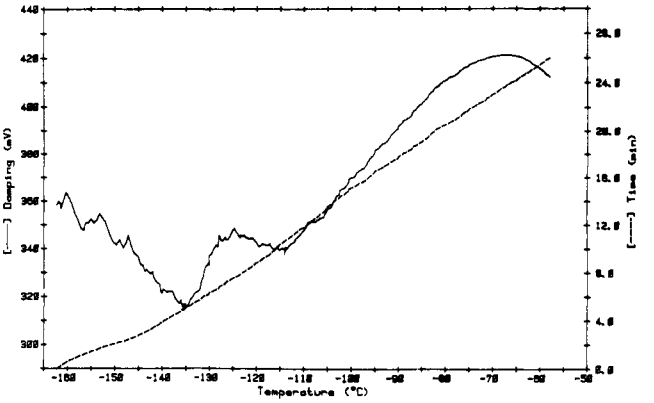

Figure 9. Dynamic mechanical analysis spectrum (20 Hz) of poly(butylene terephthalate).

The rate constants that were obtained by computer simulation of the line shapes are presented in an Arrhenius plot in Figure 8. The apparent activation energy for the pure 180° ring flip motion is 5.9 kcal/mol. This apparent activation energy is in good agreement with the theoretical calculations of Hummel and Flory[25] and of Tonelli.[26] Tonelli predicts that the barrier for phenyl rotation in poly(ethylene terephthalate) is 2 × 2.95 = 5.9 kcal/mol.[26] The rate constants obtained from deuterium NMR spectroscopy span slightly more than one order of magnitude. Frequency–temperature extrapolation of the deuterium NMR data predicts that a dynamic mechanical loss peak will occur at 20 Hz at −124 °C. The dynamic mechanical spectrum (Figure 9) shows a low-intensity peak at this temperature, consistent with a process that requires a small volume change. Although it is tempting to correlate the aromatic ring flips with this mechanical loss peak, other solid-state deuterium NMR studies on poly(butylene terephthalate)[15] show that the aliphatic groups in this polymer also have characteristic motional frequencies in this range.

Motion in the Interphase Regions. Spectra of the interphase regions can be obtained only by subtraction methods (see Figure 4). The corresponding calculated spectra are obtained by assuming that the phenyl rings in the interphase region undergo very slow 180° ring flips. The correlation time at 70 °C for a ring flip in the interphase region is approximately 8.1×10^{-6} s, whereas the correlation time for ring flips in the amorphous fraction is 1.76×10^{-6} s at this temperature. The relaxation data (see following section) are in accord with this finding.

Spin–Lattice Relaxation Data. Torchia and Szabo[12] have evaluated correlation functions to develop explicit expressions for solid-state T_1 values. Although the deuterium NMR line shape is axially symmetric (i.e., there is a one-to-one correspondence between a particular C–D bond orientation and the frequency at which it resonates), there is not a unique T_1 for each frequency. Thus, deuterium relaxation is nonexponential in general.[12] The expression for $1/T_1$ for a two-site jump is given by

$$1/T_1 = (\omega_Q^2/2)p_{eq}(1)p_{eq}(2)A_1\{g(\tau,\omega_I)[B_4 - (0.75B_1 - B_2)\cos 2\phi] + g(\tau,2\omega_I)[4B_5 - 4B_2 \cos 2\phi]\} \quad (1)$$

where

$$g(\tau,\omega) = \tau/(1 + \omega^2\tau^2)$$

$$\omega_Q = 3e^2qQ/4\hbar$$

$$\tau = (k_{12} + k_{21})^{-1}$$

$$A_1 = \sin^2 2\Theta$$

$$B_1 = \sin^2 2\theta$$

$$B_2 = \sin^4 \theta$$

$$B_4 = \cos^2 \theta + \cos^2 2\theta$$

$$B_5 = \sin^2 \theta + 0.25 \sin^2 2\theta$$

In these expressions, θ and ϕ are the polar angles that describe the orientation of the magnetic field with respect to the crystal-fixed axis system, and Θ is the angle made between the unique principal axis of the electric field gradient tensor and the flip axis. k_{12} and k_{21} describe the forward and reverse rate constants for the interconversion between sites, and $p_{eq}(1) = k_{21}/(k_{12} + k_{21})$ and $p_{eq}(2) = k_{12}/(k_{12} + k_{21})$.

The ϕ dependence of eq 1 disappears when $\theta = 0°$ (i.e., the parallel edge of the powder pattern). However, the signal-to-noise ratio suffers at this part of the pattern, primarily because of low inherent intensity, pulse power fall-off, and because the edges of the pattern are smeared out due to librational motions that occur in addition to the pure 180° flip (see previous sections). In view of these factors and because the pattern demonstrates only weak anisotropy (see Figure 7), we evaluate eq 1 at $\theta = 0°$. We use this estimated correlation time in an order-of-magnitude comparison with the correlation time obtained from line shape calculations. The correlation time at 70 °C estimated from the T_1 data is 1.6×10^{-7} s, somewhat faster than the 1.8×10^{-6} s correlation time obtained by line shape analysis for pure 180° flips. Rapid librational motions are expected to cause more efficient relaxation. This discrepancy is taken as corroborating evidence that the aromatic rings in the amorphous regions are involved in substantial motions in addition to pure 180° ring flips.

Summary

The results presented here can be used to answer and amplify on the four questions outlined in the introduction. (1) Is a pure 180° flip model adquate to explain the motion of phenyl rings in polymers? No. The phenyl rings that do flip also undergo rapid librational motions about the 1,4-phenylene axis. (2) Do the phenyl ring flips occur only in the amorphous regions? No. Our data show evidence for three motional regions. Although the phenyl rings in the crystalline region are static on the deuterium NMR time scale ($\tau_c > 10^{-3}$ s), those in the interphase regions undergo slow ($\tau_c \cong 8.1 \times 10^{-6}$ s) 180° ring flips at 70 °C. The phenyl rings in the amorphous regions undergo more rapid 180° ring flips ($\tau_c \cong 1.8 \times 10^{-6}$ s at 70 °C) superimposed on rapid librational motions. (3) What is the activation energy for the pure 180° ring flip process? We find that the apparent activation energy is 5.9 kcal/mol, in good agreement with theoretical calculations.[25,26] (4) Is there a narrow or a broad distribution of phenyl ring flip rates? The phenyl ring motions are best described by a broad envelope of phenyl ring flip rates.

Whether a phenyl ring does or does not undergo a 180° ring flip is attributed to the conformational space available to that ring. Phenyl ring excursions of 180° appear to be a universal dynamic process in solid materials, occurring in small organic molecules, biopolymers, and semicrystalline synthetic polymers. Phenyl ring flips appear to be a sensitive reporter of local morphology in the material.

References and Notes

(1) Wagner, G.; DeMarco, A.; Wüthrich, K. *Biophys. Struct. Mech.* **1976**, *2*, 139.
(2) Gall, C. M.; DiVerdi, J.; Opella, S. J. *J. Am. Chem. Soc.* **1981**, *103*, 5039.
(3) Rice, D. M.; Wittebort, R. J.; Griffin, R. G.; Meirovitch, E.; Stimson, E. R.; Meinwald, Y. C.; Freed, J. H.; Scheraga, H. A. *J. Am. Chem. Soc.* **1981**, *103*, 7707.
(4) Inglefield, P. T.; Amici, R. M.; O'Gara, J. F.; Hung, C.-C.; Jones, A. A. *Macromolecules* **1983**, *16*, 1552.
(5) Spiess, H. W. *Colloid Polym. Sci.* **1983**, *261*, 193.
(6) Garroway, A. N.; Ritchey, W. M.; Moniz, W. B. *Macromolecules* **1982**, *15*, 1051.
(7) Schaefer, J.; Sefcik, M. D.; Stejskal, E. O.; McKay, R. A.; Dixon, W. T.; Cais, R. E. *Prepr. Div. Org. Coat. Plast. Chem.* **1983**, *48*, 87.
(8) VanderHart, D. L.; Böhm, G. G. A.; Mochel, V. D. *Polym. Prepr., Am. Chem. Soc., Div. Polym. Chem.* **1981**, *22* (2), 261.
(9) A preliminary account of this work has been published. Jelinski, L. W.; Dumais, J. J.; Cholli, A. L. *Polym. Prepr., Am. Chem. Soc., Div. Polym. Chem.* **1984**, *25* (1), 348.
(10) Riande, E. *Eur. Polym. J.* **1978**, *14*, 885.
(11) Torchia, D. A. *Annu. Rev. Biophys. Bioeng.* **1984**, *13*, 125.
(12) Torchia, D. A.; Szabo, A. *J. Magn. Reson.* **1982**, *49*, 107.
(13) Wolfe, J. R., Jr. *Polym. Prepr., Am. Chem. Soc., Div. Polym. Chem.* **1978**, *19* (1), 5.
(14) 1979 Annual Book of ASTM Standards, Part 35, D 1505-68, p 482, American Society for Testing and Materials, Philadelphia, PA.
(15) Jelinski, L. W.; Dumais, J. J.; Engel, A. K. *Macromolecules* **1983**, *16*, 492.
(16) Davis, J. H.; Jeffrey, K. R.; Bloom, M.; Valic, M. I.; Higgs, T. P. *Chem. Phys. Lett.* **1976**, *42*, 390.
(17) Blinc, R.; Rutar, V.; Seliger, J.; Slak, J.; Smolej, V. *Chem. Phys. Lett.* **1977**, *48*, 576.
(18) Hentschel, R.; Spiess, H. W. *J. Magn. Reson.* **1979**, *35*, 157.
(19) Mehring, M. "High Resolution NMR in Solids", 2nd ed.; Springer-Verlag: New York, 1983.
(20) Bloom, M.; Davis, J. H.; Valic, M. I. *Can. J. Phys.* **1980**, *58*, 1510.
(21) Spiess, H. W.; Sillescu, H. *J. Magn. Reson.* **1981**, *42*, 381.
(22) Ito, M.; Kanamoto, T.; Tanaka, K.; Porter, R. S. *Macromolecules* **1981**, *14*, 1779.
(23) Kitamaru, R.; Horii, F.; Hyon, S.-H. *J. Polym. Sci., Polym. Phys. Ed.* **1977**, *15*, 821.
(24) Horii, F.; Kitamaru, R. *J. Polym. Sci., Polym. Phys. Ed.* **1978**, *16*, 265.
(25) Hummel, J. P.; Flory, P. J. *Macromolecules* **1980**, *13*, 479.
(26) Tonelli, A. E. *J. Polym. Sci., Polym. Lett. Ed.* **1973**, *11*, 441.